2010 IEEE Intelligent Vehicles Symposium
University of California, San Diego, CA, USA
June 21-24, 2010

Drivable Road Region Detection using a Single Laser Range Finder for Outdoor Patrol Robots

Youjin Shin, Changbae Jung, Woojin Chung

Abstract— For outdoor navigation, it is necessary to find the relevant features of outdoor road environments and detect drivable region for robot's motion. This paper presents a methodology for extracting the drivable road region by detecting the prominent road features and obstacles through a single laser range finder. The prominent features of roads are curbs and the road surface. The laser range finder is mounted on the mobile robot, looks down the road with a small tilt angle, and obtains two-dimensional range data. The proposed method is computationally more efficient in comparison with vision-based techniques and applicable for various road conditions in target environment. Experimental results confirm the reliability of the algorithm.

I. INTRODUCTION

Fig.1. Target Environment

Recently, outdoor patrol service robots receive much attention. Fig. 1 shows the petroleum storage facility, which is a large-scale outdoor environment. The first application task is an autonomous navigation in the road environment. A great deal of works has been carried out on outdoor navigation techniques. In particular, the extraction of the features of outdoor environments is considered to be important for reliable outdoor navigation. Recently, there have been remarkable technological breakthroughs in outdoor navigation through the well-known DARPA urban challenge. Some successful technologies can be found, for example, in [4]. Although there are several powerful solutions, most of the schemes are developed on the basis of high cost sensing equipments. Vision is the most common and popular sensing modality that is used by most researchers for road-lane detection. However, it can pose difficult challenges under bad weather or illumination change.

Other methods are based on Laser Range Finder sensors that obtain range data. Rho [5, 6] proposed an algorithm for detecting curbs by extracting the line of the road surface using Hough Transforms and determining the breakpoints of the line. The applicable area is limited to the road with curbs and the road surface should be flat enough. In [7], an algorithm is presented for detecting the line of curbs for some classes of environment using an Extended Kalman Filter .

In [17], traversable road extraction method was presented for autonomous robot navigation in outdoor cluttered pedestrian walkways. Several laser sensors were needed to implement the algorithm. Kodagoda [8-15] proposed a reliable curb detection algorithm on the basis of EKF. The algorithm was experimentally verified under the dynamic obstacle environment. In this paper, we propose the algorithm to recognize curbs and the surface of the road on the basis of a single LRF. Since the LRF should be installed in order to detect obstacles, the proposed algorithm can be applied without additional costs. The algorithm can also be used for determination of the drivable region of the road.

The rest of the paper is organized as follows. In Section II, the problem of extracting the features of road environments is addressed and an overview of the drivable road detection algorithm is presented. In Section III, experimental results are shown for various road environments to verify the proposed algorithm. In Section IV, concluding remarks are presented.

II. DRIVABLE REGION DETECTION ALGORITHM

A. System Configuration

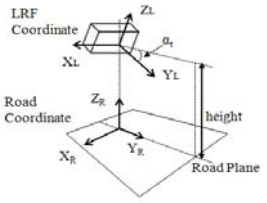

Fig.2. Sensor mounting and coordinate systems of the LRF and the road

This work were supported by Dasa Robot Corporation as a part of project "Development of Patrol and Safety Service Robot Systems" and the MKE under the Human Resources Development Program for Convergence Robot Specialists and the Ministry of Education, Science and Technology as a part of the fundamental scientific development project "Design and control of reconfigurable modular robot systems".

Youjin Shin, Changbae Jung are with school of Mechanical Engineering, Korea University, Anam-dong, Seongbuk-gu, Seoul 136-713, Korea, e-mail: (meggonagul, roka0105@korea.ac.kr).

Woojin Chung is with school of Mechanical Engineering, Korea University, Anam-dong, Seongbuk-gu, Seoul 136-713, Korea, (phone:02-3290-3375; fax:02-3290-3375; e-mail: smartrobot@korea.ac.kr).

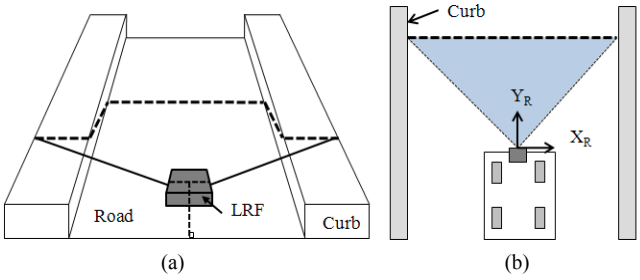

Fig.3. Ideal model of a road and curbs
(a) Dotted line : expected road data. (b) Blue area : drivable road region

The aim of this algorithm is to detect the drivable road region by extracting the road surface and curbs that are important features of the road environment. The drivable region refers to the road surface between the right and left curbs. This is achieved by a two-dimensional laser range finder sensor that looks down the road with a small tilt angle (α_t°), as shown in Fig. 3. The measurement system scans a laser spot from right to left through 180° on a plane that is inclined at an angle, α_t°. The resolution of the sensor is 1°. Fig. 2 shows the reference coordinate frames of the road and the LRF sensor. The values that will be explained for the algorithm are based on the road coordinate system. An idealized model of the environment and sensing scenario is shown in Fig. 3. As illustrated in Fig.3, the road-surface data are mostly parallel to the X_R axis. Curbs are described as straight lines that are perpendicular to the road surface.

B. Road-Feature Detection

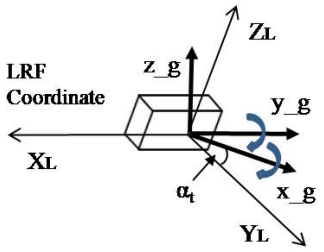

Fig.4. Coordinate systems of the LRF and Gyro-Compass (x_g, y_g, z_g) (Y_L: Direction in which the robot is headed, Pitch angle α: rotation around the X_L axis, Roll angle β is the rotation around the Y_L axis.)

The laser range finder is mounted on the robot and looks down with a small tilt angle α_t°. The tilt angle is selected on the assumption that the robot is on a flat surface. The tilt angle should be compensated when the robot moves on irregular surfaces like speed humps. Therefore, in this study, a gyro-compass sensor was used to monitor pitch angle α and the roll angle β. The coordinate systems of a gyro-compass and a laser range finder are shown in Fig. 4.

$$R_{Xr} = \begin{pmatrix} 1 & 0 & 0 \\ 0 & \cos(-\alpha) & -\sin(-\alpha) \\ 0 & \sin(-\alpha) & \cos(-\alpha) \end{pmatrix} \quad (1)$$

$$R_{Yr} = \begin{pmatrix} \cos(\beta) & 0 & \sin(\beta) \\ 0 & 1 & 0 \\ -\sin(\beta) & 0 & \cos(\beta) \end{pmatrix} \quad (2)$$

$$R = R_{Yr} \cdot R_{Xr} \quad (3)$$

The laser data are expressed in the road coordinate by the rotation matrix given by eqs. (1) - (3). The variance of the robot's tilt angle on the experimental road surface is 0.75°. In order to cope with experimental oscillation of tilt angle α_t, the tolerance of α_t is determined as $\varepsilon = 2°$.

The expected range of the road surface in road coordinate is shown in Fig. 5. This region is determined by considering the height of the LRF and ε. First, LRF data that are in this range are extracted. Then, consecutive road data are computed from the extracted data to compute the gradient. The range data are classified as the road surface when the gradient is parallel to the X_R axis. Finally, the consecutive extracted data are used for defining the road-feature, i.e., the line properties (angle: θ_f, distance: ρ_f). The road-feature detection algorithm can be summarized as follows.

Algorithm 1: Computing the Road-Feature Properties
Input: ε, θ_e (45°, Expected gradient of the road surface)

1. Set the expected range of the road using ε (shown in Fig. 5)
2. While i ≤179 do
   if LRF $y_i \subset$ Y_range
      if LRF $z_i \subset$ Z_range
         if the gradient (θ) of the line of three consecutive data (x_{i-1}, x_i, x_{i+1}, y_{i-1}, y_i, y_{i+1}) by least square method ≤ Gradient (θ_e)
         Select x_i , y_i , z_i as the road
3. Return θ_f, ρ_f, f_height (properties of consecutive road datasets)

θ_e (= 45°) is the experimental value determined from experiences. The extracted information of the road-surface (θ_f, ρ_f) is shown in Fig. 6 and the line is computed from the conventional least square method. θ_f is used for curb detection. The reason why we detect the height of the field (f_height) is that we need to know the height to determine the drivable region in terms of its height. Even if we know the robot pose using the gyro-compass sensor, the measurement is subject to errors. Fig. 6 indicates that the robot leans to the right and that the LRF data do not match our expectation that is shown in Fig. 3 with regard to an ideal road model.

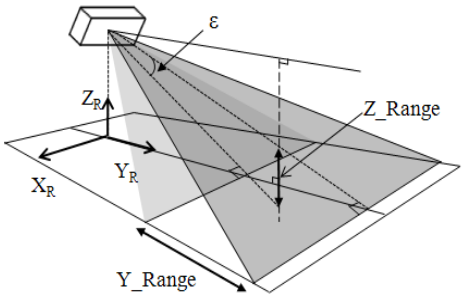

Fig.5. Detectable region of the road surface

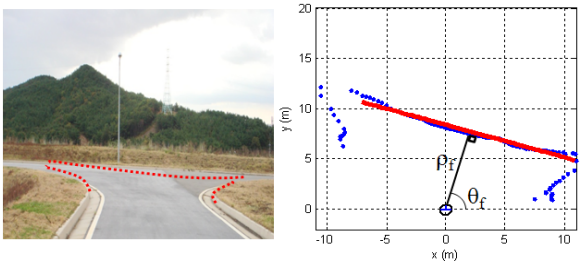

Fig.6. Results of Road-Feature Detection (θ_f, ρ_f)

C. Curb Detection

Through experiments conducted in this paper, curbs are extracted as a line that is composed of at least three points. Therefore, it is difficult to extract the correct curb lines under various road conditions. In our study, we define several attributes that properly describe the curb features. The defined attributes are shown below.

Att_1. The difference between curb orientation θ_c and θ_f is normally 90°. In most cases, $|\theta_c - \theta_f| \geq 30°$
Att_2. The difference between ρ_f and the maximum y data of the curb is nearly zero, as shown in Fig. 3,
dif_dist (m) ≈ 0
Att_3. The difference of curb orientations is nearly zero and under 10°, dif_theta (°) ≈ 0
Att_4. The road width is known and it is nearly equal to the distance between curbs, dist_width (m) ≈ 0

It is commonly assumed that the robot's heading is parallel with the curb orientation, for example, in [9]. However, this assumption becomes invalid when there is an inclination of the road surface.

The experimental results of $|\theta_c - \theta_f|$ are shown in Fig. 7. This test was performed while the robot traveled around the area marked in Fig. 1. The number of acquired range images was about 2000. The mean value of angular difference, $|\theta_c - \theta_f|$, was about 90° and the minimum difference was 36°. On the basis of this result, Att_1 is defined.

Att_1 extracts the candidate lines of both right and left curbs. Att_2, 3 and 4 add more constraints. Eq. (4) shows this process.

$$Curb\_Choice = G1 \cdot dist\_width + G2 \cdot dif\_theta \cdot 0.1 + G3 \cdot dif\_dist \quad (4)$$

In practice, Curb-Choice in eq. (4) was mostly smaller than 5 for curbs. For other line features except for the curbs, Curb-Choice was greater than 10. G1, G2, and G3 are the weights of attributes. We used 1, 2, and 1 from experiences. The angle, distance values (θ_c, ρ_c), and data range of the detected curbs are extracted as a result of the curb-detection algorithm.

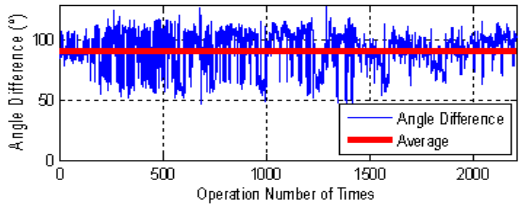

Fig.7. Properties of the angular difference between the road-surface line and the curb line, $|\theta_c - \theta_f|$

D. Drivable Region and Obstacle Detection

The detection of the drivable road region is based on the result from road-feature detection and curb detection. First, the expected region of the drivable area is defined. The drivable region refers to the road surface between the right and left curbs. Therefore, we extract the LRF data that belongs to this range and close to ρ_f. Then, drivability is determined by the height because the drivable region must have a small elevation f_height. Lastly, we gate data that have a similar gradient with θ_f. The range of the drivable region and its coordinates (X_{pass}, Y_{pass}) are obtained as follows.

Algorithm 2: Detect the Drivable Road Region
Input: θ_f, ρ_f (properties of the road-feature line), r_width, l_width (curb position based on the ρ_c value), f_height (height of the road surface)

1. Set the expected range of the drivable road region
   A. X_Range2: range between r_width and l_width
   B. Y_Range2: range around ρ_f
   C. Z_Range2: f_height ± r (r: drivable height limit)
2. While i ≤ 179 do
   if LRF $x_i \subset$ X_Range2
   if LRF $y_i \subset$ Y_Range2
   if LRF $z_i \subset$ Z_Range2
   if the gradient (θ) of the line of three consecutive data (x_{i-1}, x_i, x_{i+1}, y_{i-1}, y_i, y_{i+1}) by least square method ≈ Gradient (θ_f)
   Select x_i , y_i , z_i
3. Return X_{pass}, Y_{pass} (LRF data of Drivable Region)

The consecutive data of the drivable road region are classified into one group and termed as 'Valley,' which is used to determine drivable area in Vector Field Histogram algorithm (VFH) [16]. The drivable road region is restricted by tilt angle α_t°. The overview of the proposed algorithm is summarized in Fig. 8.

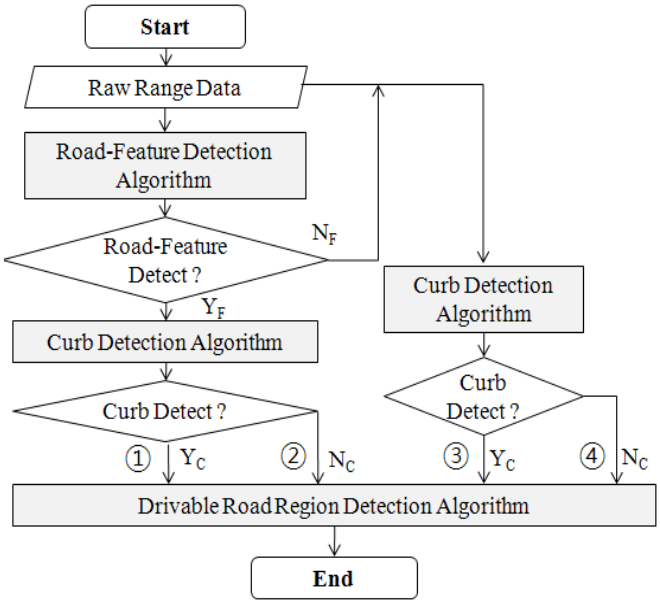

Fig.8. Flowchart of the algorithm

III. Experimental Results

A. Experimental Setup

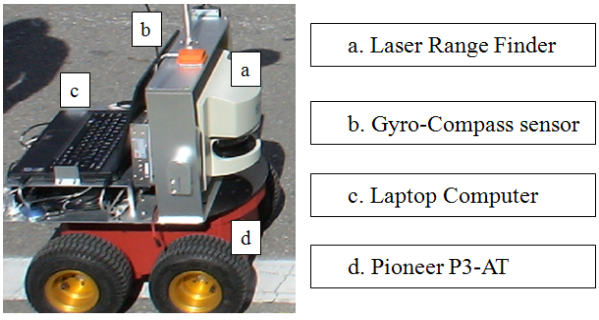

Fig.9. Robot platform

Fig.9 shows the experimental setup. A SICK laser sensor is mounted on this robot for detecting the range around the robot. The maximum range of the LRF is 33m and its static error is under 0.3cm. To detect the road surface and curbs, the LRF was mounted with small tilt angle α_t. We also used the angular value from the gyro-compass sensor to detect the pose of the robot while the robot was in motion.

B. Algorithm Validation

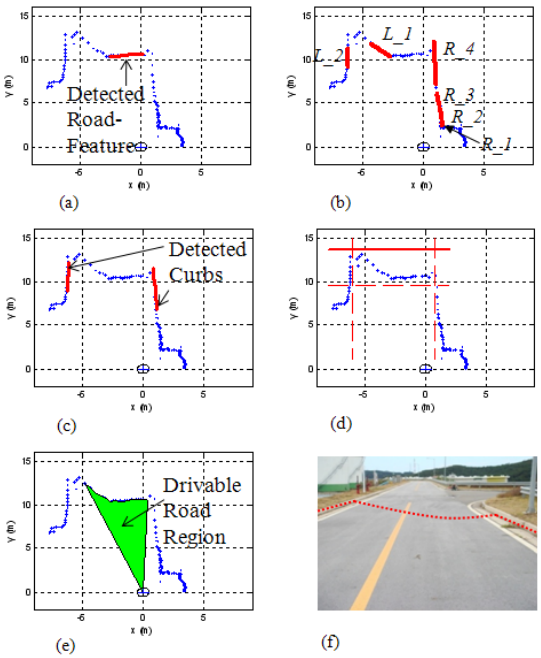

Fig.10. Data extraction due to the algorithmic process and the actual environment

TABLE I
SELECTION OF CURBS (VALUES RESULTING FROM EQ. (4))

	R_1	*R_2*	*R_3*	*R_4*
L_1	19.1	20.1	13.4	13.4
L_2	10.9	9.9	9.8	3.1

Fig. 10 shows the algorithmic process using laser data at each stage and the ensuing results. The experimental environment is indicated in Fig. 10(f) and the red dotted line denotes LRF data in a real environment. In Fig. 10(a), the dots refer to actual LRF data and the line is the result of road-feature detection (θ_f = 95.8°, ρ_f = 10.5m, f_height = -0.09m). The six red lines shown in Fig. 10(b) are the curb candidates that are extracted through the angular difference with respect to the road-surface (Att_1.). There are four right-curb candidates and two left-curb candidates. Then, the detected curbs are selected by the comparing right and left curb pairs using eq. (4). The values that result from eq. (4) are shown in TABLE I. The detected curbs are indicated in Fig. 10(c). In Fig. 10(d), the selected range using the above results is described by dotted red lines. By considering this range, the drivable road region is shown in Fig. 10(e).

As shown in Fig. 11, the results of curb detection and drivable road detection are compared with the actual values. The detected curbs are accurate with small errors of under 0.5° for the angle and 0.1m for the distance in the road coordinate. The actual drivable region is within [86°, 116°] and the detected drivable region is within [86°, 114°] with an error of 2°, which is negligible for outdoor motion control.

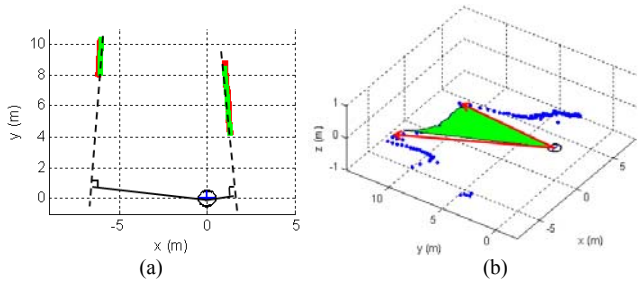

(a) (b)

Fig.11. (a) Results of curb detection (green line: actual curb; red line: detected curb). (b) Results of the detection of the drivable road region (green area: detected region; red arrow: actual region)

C. Various Road Conditions

We verified our algorithm through experiments with various road environments. The experimental results are shown in Fig. 12. Fig. 12(a) shows one road condition with a convex road surface and a road-width of 7m. In this condition, the range data can detect only the right curb and the LRF is tilted by 2.5°. Another road condition is indicated in Fig. 12(b) with a flat road surface and a road-width of 5m. In this condition, the range data can detect both right and left curbs and the LRF is tilted by 5.5°.

The figures on the left in Fig. 12 are experimental environments. Various information is shown in the figures on the left: the robot position; LRF data on the real environment (red dotted line); and the expected drivable region (green arrow). As shown in the figures on the right in Fig. 12, the detected drivable road region well coincides with the expected drivable region that is shown in the figures on the left. The detected road-feature values are shown in the figures on the right.

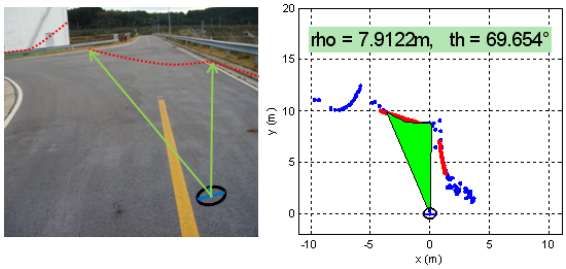

(a) Environment ①: convex road surface (road_width = 7m, α_t = 2.5°)

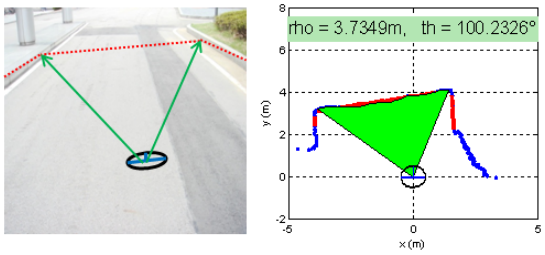

(b) Environment ②: flat road surface (road_width = 5m, α_t = 5.5°)

Fig.12. Experimental results for various road conditions

D. Obstacles

We tested with obstacles and speed humps. The experimental results are indicated in Fig. 13. Fig. 13(a) shows one road condition with an obstacle (box) on the left side of the robot, while the robot is looking upward as it climbs up the speed hump. In this condition, range data alone cannot detect curbs and the LRF is tilted by 5.5°. Fig. 13(b) shows another road condition with an obstacle (box) on the left side of the robot, while the robot is looking downward the road as it climbs down the speed hump. In this condition, range data alone cannot detect curbs and the LRF is tilted by 5.5°. This experiment was performed based on the algorithm that is indicated in Eq. (3). In this situation, the key issue is where the road-surface data are positioned in terms of road coordinates. The result with regard to the distance of the road surface is about 8m in Fig. 13(a) and 2m in Fig. 13(b). In other words, road-feature detection works properly and the range selection process is successful using the pose angle of the robot from the gyro-compass sensor.

Various information is shown in the figures on the left that denote the robot position, LRF data on the real environment (red dotted line), and the expected drivable region (green arrow). As shown in the figures on the right in Fig. 13, the detected drivable road region well coincides with the expected drivable region from the figures on the left. The robot can distinguish obstacles from the road surface and detect the drivable region that does not include obstacles.

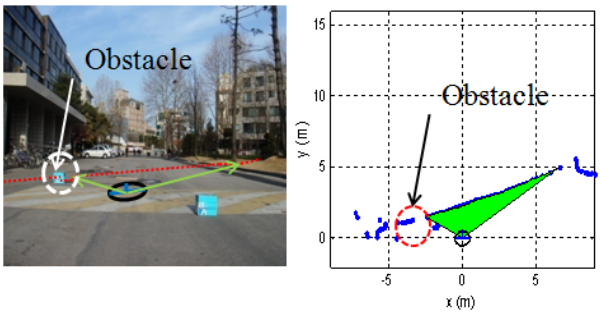

(a) Environment ③: obstacle (pitch_angle = -2.29°, α_t = 5.5°)

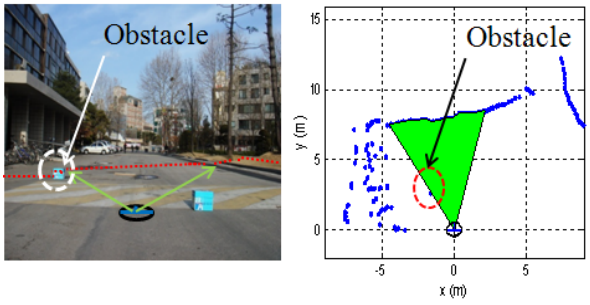

(b) Environment ④: obstacle (pitch_angle = 5.57°, α_t = 5.5°)

Fig.13. Experimental results for various road conditions

E. Reliability of the Algorithm

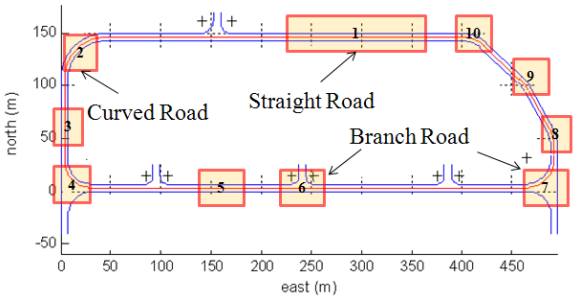

Fig.14. Target road environment that has various road conditions (curved roads, straight roads, branch roads), a sector of the given area that is shown in Fig. 1

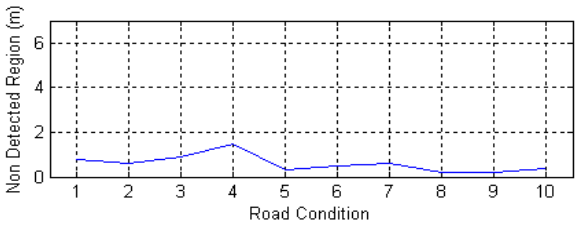

Fig.15. Missed drivable road region

To confirm the reliability of the algorithm, the experiment was performed in the area that is shown in Fig. 14. In this experiment, the robot navigates for about 1km and receives about 3000 laser scans for one run. The experiment takes about an hour. The laser range finder is tilted by 2.5°. As shown in Fig. 14, this environment contains various road conditions such as straight, curved, and branch roads.

In Fig.15, missed drivable road region is shown. The drivable road region is constant as road-width of 7m in this experiment. The detected drivable road region is also defined as a detected road-width. The difference between the real and detected drivable road region for the indicated region in Fig.14 is shown in Fig.15. The result means that the error of the drivable road detection algorithm is under 1m and it is reliable for the robot to navigate on the road environments.

IV. Conclusion

In this paper, we proposed a method that can address perceptual issues with regard to outdoor road environments for outdoor navigation. We use a single laser range finder to detect curbs, road-surfaces, and obstacles. Hence, this method can be easily adopted for practical applications. By extracting two types of information (on curbs and road-surfaces), we increase the reliability of drivable road detection in relation to the findings of other studies. As a result, this method has been verified by experiments for various road environments. This algorithm is computationally efficient and guarantees the safety of outdoor navigation.

References

[1] Wang Rongben, Xu, Libin Youchun, Zhao Yufan, "A vision-based road edge detection algorithm", IEEE Intelligent Vehicle Symposium, vol.1, pp.141-147, June 2002.

[2] Truong Quoc Bao, Lee Gyung Ryong, Heo Nam Geon, Yum Young Jin, Kim Jong Gook, "Lane Boundaries Detection Algorithm Using Vector Lane Concept", International Conference on Control, Automation, Robotics and Vision (ICARCV'08), Vietnam.

[3] Wu Bing-Fei, &Lin Chuan-Tsai, "Robust Lane Detection and Tracking for Driving Assistance Systems", IEEE International Conference on Systems, Man and Cybernetics (SMC'07), Canada.

[4] Dahlkamp H., Kaehler, A., Stavens, D., Thrun, S., & Bradski, G., "Self-supervised Monocular Road Detection in Desert Terrain", Robotics Science and Systems, Philadelphia, PA, USA, August 2006.

[5] Roh Chi-Won, Kim Seung-Hun, Kim Moon-June, Kang Sung-Chul, Hong Suk-Kyo, "Development of Patrol Robot using DGPS and Curb Detection", International Journal of Control, Automation and Systems, vol.13,pp.140-146, 2007.

[6] Kim Seung-Hun, Roh Chi-Won, Kang Sung-Chul, &Mignon Park, "Curb Detection Using Laser Range Rinder for Reliable Ourdoor Navigation", Proceedings of IEEE International Conference on Advanced Robotics (ICAR'07), pp.930-935, South Korea.

[7] Yu Chunhe, & Zhang Danping, "Road Curbs Detection Based on Laser Radar", Proceedings of IEEE International Conference on Signal Processing (ICSP'06), China.

[8] Kodagoda K. R. S., Ge Shuzhi Sam, Wijesoma W.S.,& Balasuriya A. P., "IMMPDAF Approach for Road-Boundary Tracking", IEEE Trans. Veh. Technol., vol.56, pp.478-486, March 2007.

[9] Wijesoma W. S., Kodagoda K. R. S., & Balasuriya A. P., " Road-Boundary Detection and Tracking Using Ladar Sensing", IEEE Trans. Robot. Automat. vol. 20, pp.456-464, June 2004.

[10] Wijesoma W. S., Kodagoda K. R. S., & Balasuriya A. P., "A Laser and a Camera for Mobile Robot Navigation", Proceedings of IEEE International Conference on Control, Automation, Robotics And Vision (ICARCV'02), pp.740-745, Singapore

[11] Wijesoma W. S., Kodagoda K. R. S., & Balasuriya A. P., "Road Feature Extraction using a 2D LMS", Proceedings of IEEE International Conference on Control, Automation, Robotics And Vision (ICARCV'02), pp.453-458, Singapore

[12] Kodagoda K. R. S., Wijesoma W. S., & Balasuriya A. P., "Road Curb and Intersection Detection using a 2D LMS", Proceedings of the IEEE/RSJ International Conference on Intelligent Robots and Systems(IROS 2002), pp.19-24, Switzerland

[13] Wijesoma W. S., Kodagoda K. R. S., & Balasuriya A. P, "Laser and Vision Sensing for Road Detection and Reconstruction", Proceedings of IEEE 5th International Conference on Intelligent Transportation Systems (ITSC 2002), pp.248-253, Singapore.

[14] Wijesoma W. S., Kodagoda K. R. S., Balasuriya A. P, & Teoh E. K., "Road Edge and Land Boundary Detection using Laser and Vision", to appear in Procs. Of IEEE/RSJ International Conference on Intelligent Robots and Systems (IROS 2001), pp.1440-1445, USA.

[15] W. S., Kodagoda K. R. S., Balasuriya A. P, & Teoh E. K., "Laser and Camera for Road Edge and Mid-line Detection", Proceedings of the Second International Workshop on Robot Motion and Control, RoMoCo'01, Poland, October 2001, pp269-274.

[16] Borenstein J., & Koren Y., "The Vector Field Histogram – Fast Obstacle Avoidance for Mobile Robots" IEEE Journal of Robotics and Automation, vol. 7, No 3, June 1991, pp. 278-288C. J. Kaufman, Rocky Mountain Research Lab., Boulder, CO, private communication, May 1995.

[17] Morales Yoichi, Carballo Alexander, Takeuchi Eijiro, Aburadani Atsushi, & Tsubouchi Takashi, "Autonomous Robot Navigation in Outdoor Cluttered Pedestrian Walkways", Journal of Field Robotics, vol. 26, pp. 609-635 (2009)